Published by :
http://www.ijert.org

International Journal of Engineering Research & Technology (IJERT)
ISSN: 2278-0181
Vol. 9 Issue 05, May-2020

Computational Analysis of Winglet-Rudder Configuration for Crosswind Landing

[1]V. Yamini Anoosha, [2]Ruchi Saraf, [3]Prakriti Bhowmick, [4]Sowndarya, [5]Supritha C L,
[1] Asst Professor, Department of Aeronautical Engineering, Dayananda Sagar College of Engineering, Bengaluru, India.
[2,3,4,5]Student, Department of Aeronautical Engineering, Dayananda Sagar College of Engineering, Bengaluru, India.

Abstract:- **The need for improving the aerodynamic efficiency and maneuvering capabilities of the aircraft during crosswinds has been of prime importance in the field of aviation. The main objective of the project is to further improve upon these two parameters. The configuration used for analysis consists of AIRBUS A320 NEO aircraft with provisions for modifications. Additional Winglet-Rudder configurations have been introduced in the winglet section of the aircraft model. An approach speed of 140 knots is considered. Further research is done by using an optimized winglet-rudder configuration for different crosswind velocities- 30 knots and 50 knots. The introduction of the winglet rudder configuration further decreases the net yaw moment enabling an easy maneuver over the aircraft and also ensuring a safe landing during this critical landing condition.**

Keywords- Winglet-rudder configuration, Crosswind landing, Crabbing technique.

I. INTRODUCTION

It's a well-known fact that the main responsibility which puts the pilot's skill under test is while landing. The pilots face many unfavorable conditions such as adverse yaw, structural damage, zero visibility, crosswind conditions, and so on. The most severe and undesirable condition while landing is the crosswind condition.

Rudder is the primary control surface responsible for yawing moment when deflected and it also provides directional stability to the aircraft. In severe landing conditions like a crosswind, the rudder is of prime importance. The crosswind velocities are sometimes too harsh that the rudder deflection won't be sufficient. In such instances, this paper focuses on proving the effects of winglet-rudder which helps the aircraft to overcome this condition and aim for a safer landing.

There are many techniques currently in use to overcome this type of landing and one of the most prominent techniques used is the crabbing technique; which is also preferred by many pilots. The aircraft is inclined at a certain angle with respect to the runway mid-line (crab angle) while simultaneously operating the rudder to reduce the yaw moment which enables safe landing.

In this paper we are considering AIRBUS A320 NEO which has been modified by incorporating a rudder in the winglet section of the aircraft. The main rudder when operated along with the winglet-rudder should be able to provide the required moment to overcome the crosswind. According to The Federal Aviation Administration (FAA), the standard crosswind condition which any commercial aircraft should be able to handle is 30knots. In this experiment we are considering both 30knots which is a standard crosswind velocity and 50knots which is a severe crosswind velocity to check the effects of the main rudder along with the winglet-rudder on the net force to ensure a safe landing. The geometry of AIRBUS A320 NEO is created using CREO 5.0 software and the dimensions are obtained from the Airbus website. The analysis is performed using ANSYS FLUENT 2019 R2 for each case which will be explained further in this paper. Initially, code verification is done for the solver to prove if the output is legitimate in comparison with a standard paper.

II. CODE VERIFICATION

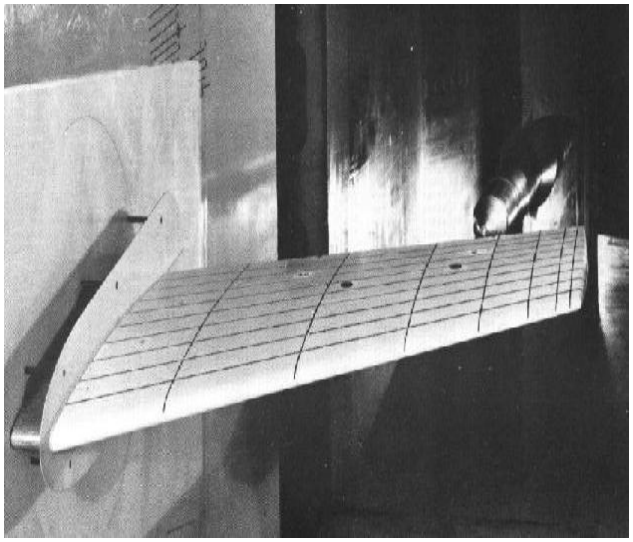

Fig 1. The Onera M8 wing.

NASA Verification and Validation Archive has offered various cases that correspond to the geometric configuration and flow condition studies which can be considered for validation of the numerical solver Fluent. The simple geometry combined with complexities of transonic flow, the Onera M6 wing is a typical CFD validation case for external flows. Many researchers have used this CFD study as a validation case in their research to check their solver fluent.
With reference to the chosen journal paper, the analysis of the ONERA wing is performed. The results obtained from this experiment should be nearer to the output of the journal paper. The results represent the efficiency of the solver fluent which will be used for our experiment.

International Journal of Engineering Research & Technology (IJERT)
ISSN: 2278-0181
Vol. 9 Issue 05, May-2020

A. *GEOMETRY LAYOUT*

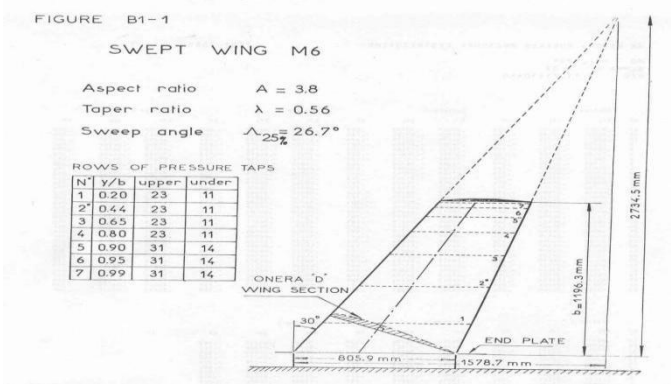

Fig 2. Geometric layout of the Onera M6 wing.

The ONERA M6 wing is a semi-span, swept-wing with no twist. It uses symmetric airfoil using the ONERA D section. The coordinates of the aerofoil indicate that there is a finite thickness to the trailing edge. For CFD simulations, an approximation is usually made of a zero trailing edge thickness.

TABLE 1: Flow conditions for scaled wing geometry.

Flow Conditions	
Mach	0.8395
Reynolds Number	11.72E+06
Angle of Attack(degrees)	3.06
The angle of side-slip(degrees)	0.0
Pressure(psi)	45.82
Temperature (R)	460.0

The CFD simulations use the flow field conditions of the above-given table1. Corresponding to a Reynolds number of 11.72 million based on the mean aerodynamic chord of 0.64607 meters.

TABLE 2: Scaled wing geometry.

Scaled wing geometry	
Span, b	1 foot
Root chord	0.6730 feet
Tip chord	0.37 feet
Taper Ratio	0.562
Leading-edge sweep	30.0 degrees
Trailing-edge sweep	15.8 degrees

Onera M6 wing geometry dimensions are scaled down to one-third of the original geometry to reduce the computational time while performing the analysis.

B. *DOMAIN*

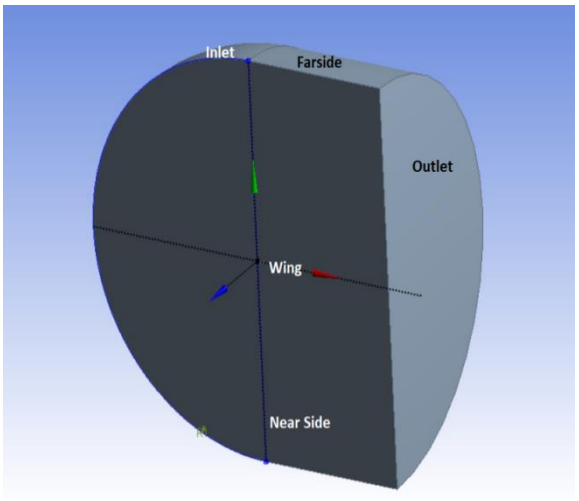

Fig 3. Fluid domain boundary.

The parts of the domain and the target body are names as given in figure 3. The near side of the domain is symmetry and the wing has a no-slip wall.

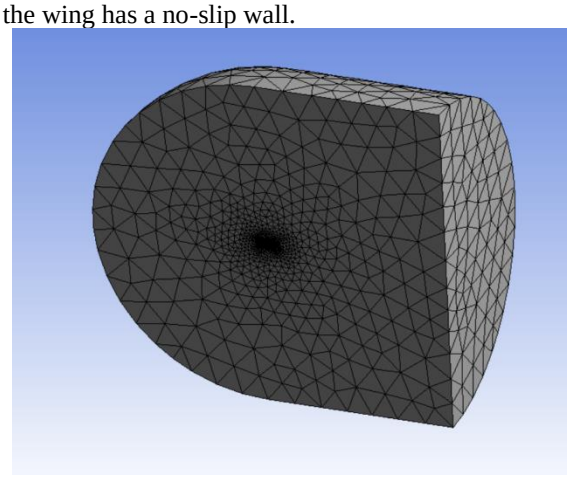

Fig 4. The meshed model of the domain.

As this is a mesh independent study, the meshing of the domain is done twice.
In the first case, the number of elements obtained is 360895. The second mesh consists of 652384 elements. The set-up details for this case are pressure-based and also a steady solver. The viscous model appropriate for this case are Spalart – Allmaras and the Energy Equation. For the easy conversion of the differential equations to the algebraic equations coupled scheme, second-order Spatial Discretization and Pseudo Transient Simulation are chosen.

International Journal of Engineering Research & Technology (IJERT)
ISSN: 2278-0181
Vol. 9 Issue 05, May-2020

C. CONVERGENCE

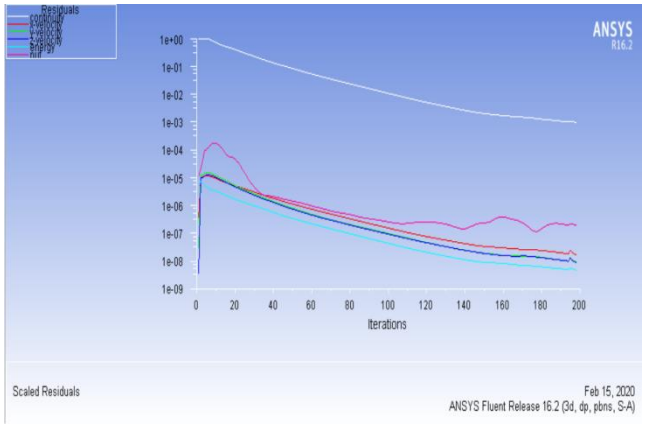

Fig 5. The convergence graph.

The above graph represents the convergence of the continuity, force, and energy equations which were run for about 200 iterations.

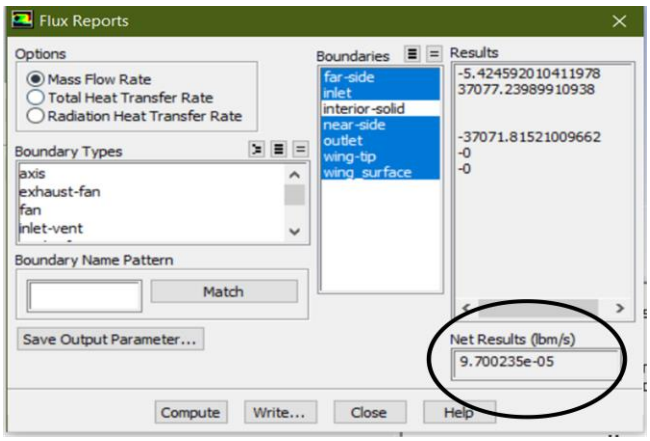

Fig 6. Conservation of mass.

One of the reports which represents the mass conservation is shown and in the figure. The mass conservation is satisfied and the net mass flow rate is negligibly small.

D. COMPARISION OF RESULTS

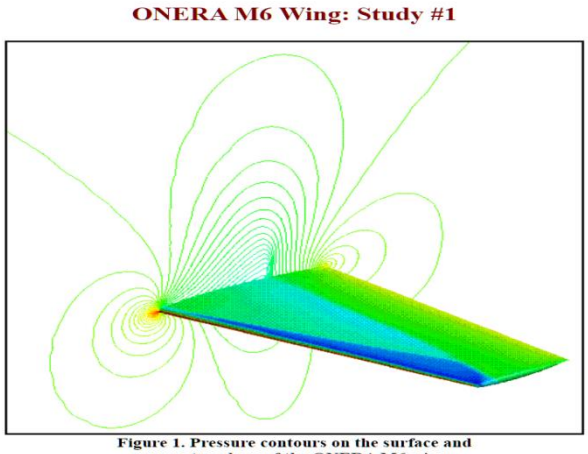

Fig 7. Mani,m,j.a ladd,a.b. Cain, and r.h.bush, “an assessment of one-and two-equation turbulence models for internal and external flows”, AIAA 97-2010, june1997.

The above figure 7. represents the pressure coefficient obtained from the journal paper mani, m., j.a. ladd, a.b. cain, and r.h. bush, "an assessment of one- and two-equation turbulence models for internal and external flows", aiaa 97-2010, June 1997.

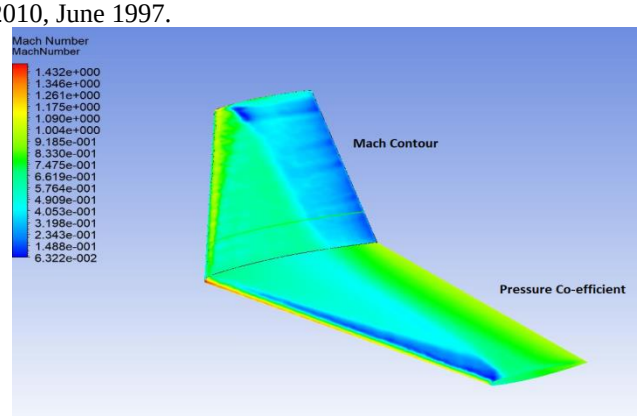

Fig 8. Mach and pressure contours of mesh 1.

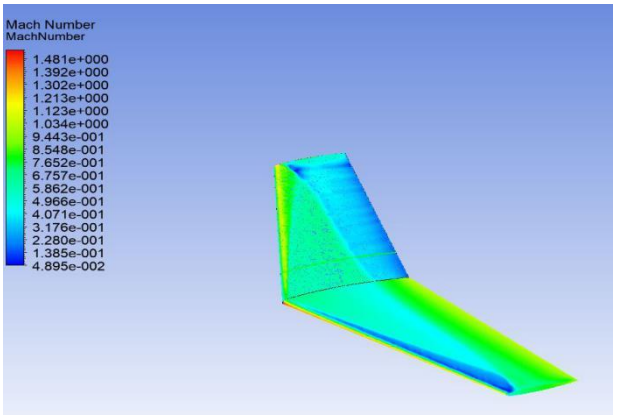

Fig 9. Mach and pressure contours of mesh 2.

The above contours represent the Mach and the pressure contours over the Onera M6 wing of the mesh 1 and mesh 2. The color scheme displays the maximum and minimum effects of these two parameters. This proves that the solver fluent used in this experiment is providing legitimate results.

E. RESULTS

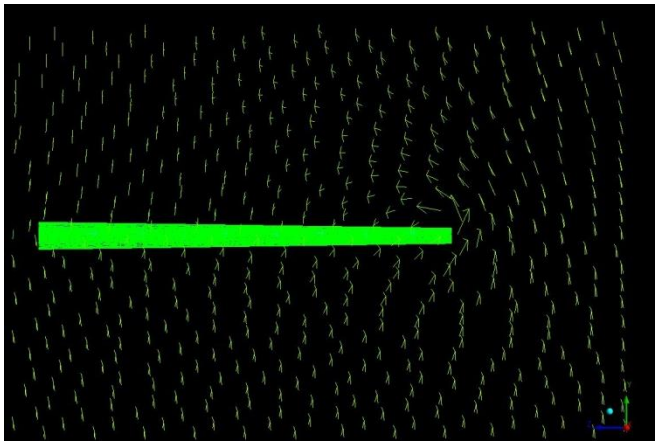

Fig 10. Tip vortices of mesh1 model.

International Journal of Engineering Research & Technology (IJERT)
ISSN: 2278-0181
Vol. 9 Issue 05, May-2020

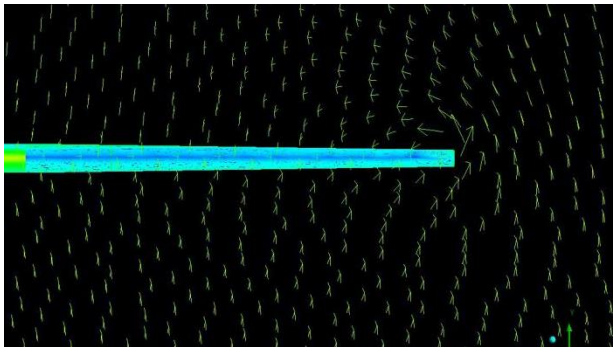

Fig 11. vortices of mesh 1 model.

The tip vortices of the mesh 1 and mesh 2 models are extracted for comparison. The mesh model 2 shows the improved accuracy over the mesh 1 model.

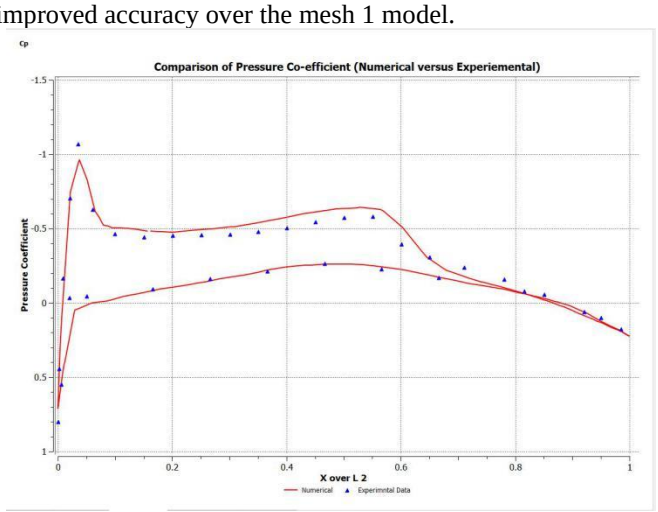

Fig 12. numerical vs experimental graphs for mesh model 1.

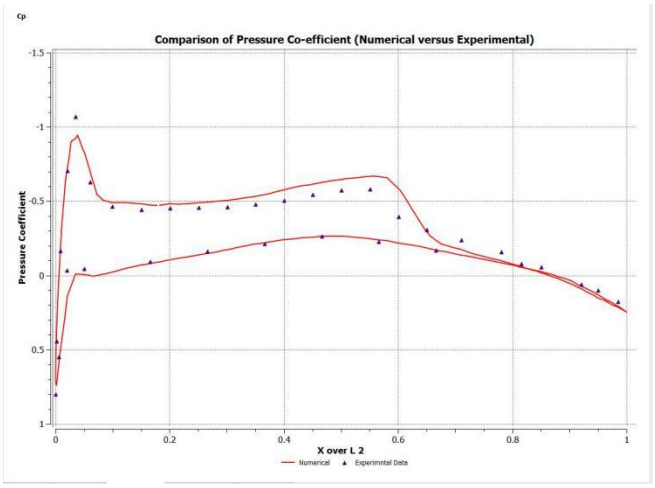

Fig 13. numerical vs experimental graphs for mesh model 2.

The above figures 13. and 14. represents the curves of numerical and experimental solutions for mesh model 1 and 2 respectively.

TABLE 3: Lift and drag comparison.

Lift and drag comparison		
	CL	***CD***
NASA	0.1410	0.0088
MESH 1	0.1271	0.0110
MESH 2	0.1292	0.0100

The above-given Table 3. indicates that the lift and drag values obtained from the solver fluent and the values from the NASA website is approximately closer. Thus the solver is suitable to conduct further analysis effectively.

III. THEORETICAL BACKGROUND

In all types of aircraft, one of the most significant roles of the rudder is to maintain safe landing while a crosswind is blowing. The rudder helps the aircraft's nose to align itself to the mid-line of the runway. The force created by the wind is counteracted by the employment of the rudder. The rudder creates a crab angle (ϭ) which prevents the aircraft from drifting away from the runway. The rudder of the aircraft should be designed carefully to overcome the crosswind for some particular crab angle. The approach velocity (VT) of AIRBUS A320 NEO, in this case, is 140 knots. The crosswind velocity (VW) approaching the aircraft is 30 knots, which is considered to be the standard crosswind velocity which any commercial aircraft should be able to withstand. The extreme crosswind velocity considered in this case that cannot to handled by the aircraft is 50 knots. Analysis is performed for various cases for each 30 and 50 knots to prove the efficiency of the winglet-rudder along with the main rudder.

The crab angle, approach velocity, and the crosswind velocity are dependant on each other. The crab angle for a particular crosswind velocity should be achieved by a certain deflection of the rudder.

The formula to determine the crab angle for a certain crosswind velocity for the approach velocity 140 knots is given below.

$$Ϭ= \sin^{-1}(\frac{VW}{VT}) \text{……..Eqn 2.1}$$

Ϭ= Crab angle.
VW= Crosswind velocity (30 and 50 knots)
VT= Approach velocity (140 knots)

TABLE 4: Crab angle and rudder deflections for crosswind velocities.

Approach velocity (knots)	140	140
Crosswind velocity (knots)	30	50
Crab angle (degrees)	12.37	20.92
Rudder deflection (degrees)	24 and 30	24 and 30

Table 4. gives us the crab angle and rudder deflections for 30 and 50 knots with the approach velocity of 140 knots. These angles will be considered for the analysis of each case.

IV. GEOMETRY

The CAD model of the AIRBUS A320 NEO is created using CREO 5.0 software. The dimensions are obtained from the Airbus website. In the winglet part of the wing, rudders are incorporated.

International Journal of Engineering Research & Technology (IJERT)
ISSN: 2278-0181
Vol. 9 Issue 05, May-2020

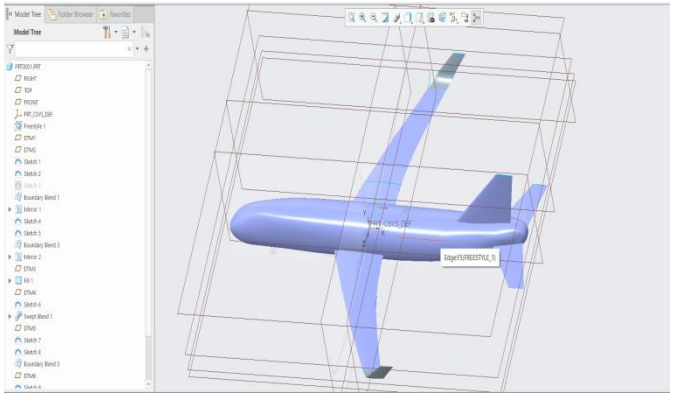

Fig 14. CAD model of Airbus A320 NEO.

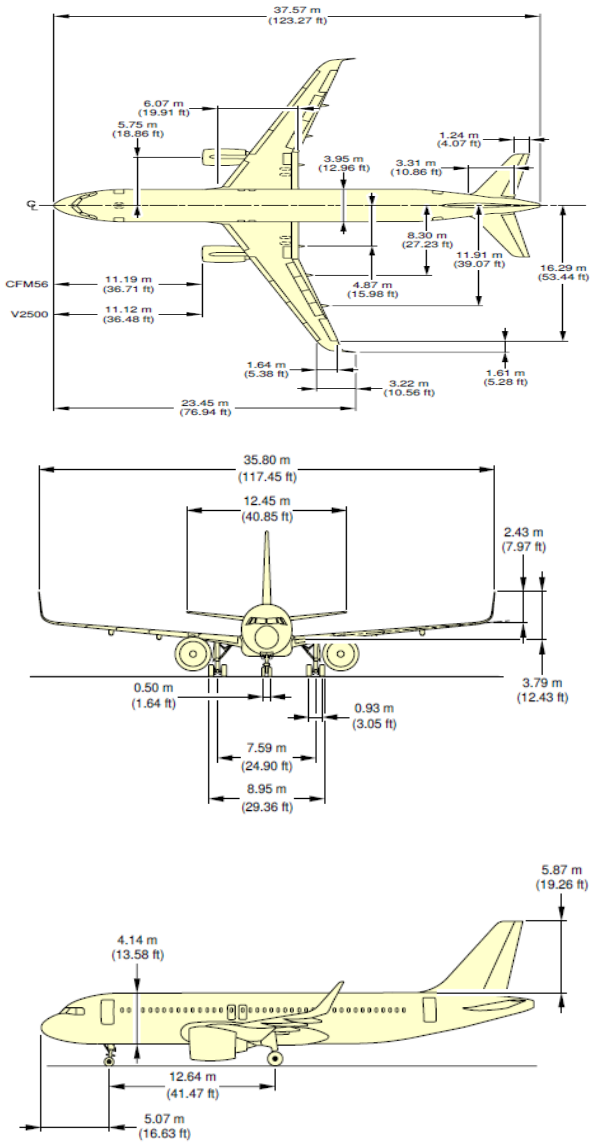

Fig 15. Airbus A320 NEO.

The dimensions of the AIRBUS A320 NEO are taken from the Airbus manual on the Airbus website. The CAD model of the aircraft for this experiment is based on these dimensions. As the aircraft is a huge vehicle and the dimensions are in meters, the exact dimensions were scaled down to 35:1 ratio. This helps in reducing the computational time while performing the analysis.

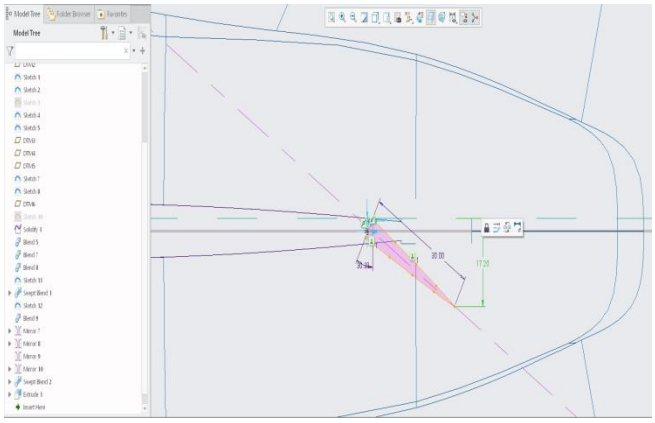

Fig 16. Main rudder deflection.

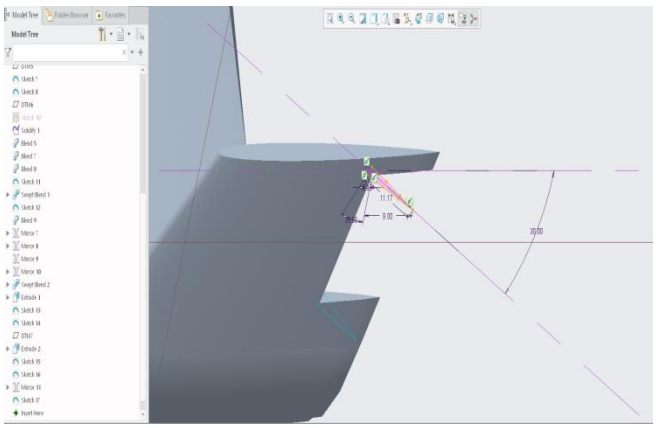

Fig 17. Winglet-rudder deflection.

The above figure 14 and 17 shows the main rudder deflection and the deflection of the winglet-rudder respectively using CREO 5.0 software.

TABLE 5:Dimensions of the wing and the rudder.

Projected side area(Ss)	178 sq.m
Wing area(S)	122.6 sq.m
Wingspan(b)	34.09m
Vertical tail span(bv)	5.87m
Vertical tail arm(lv)	12.53m
Vertical tail area(Sv)	21.50m

Tables 5. represent the dimensions used to create the modified winglet-rudder configuration of AIRBUS A320 NEO using CREO 5.0.

International Journal of Engineering Research & Technology (IJERT)
ISSN: 2278-0181
Vol. 9 Issue 05, May-2020

V. PROCEDURE FOR ANALYSIS

The aircraft model is imported to ANSYS 2019 R2 software and the domain is created. The Boolean is created for the domain and the aircraft model. The aircraft model is then meshed.

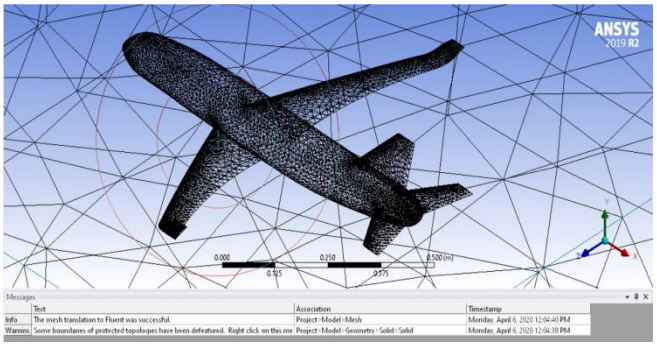

Fig 18. Meshed body of the aircraft.

Details of "Mesh"

Display	
Display Style	Use Geometry Setting
Defaults	
Physics Preference	CFD
Solver Preference	Fluent
Element Order	Linear
Element Size	Default (0.2865 m)
Export Format	Standard
Export Preview Surface Mesh	No
Sizing	
Quality	
Inflation	
Assembly Meshing	
Advanced	
Statistics	
Nodes	101744
Elements	574870

Fig 19. Details of the mesh.

Figures 17. and 18. provide the mesh details of the models. The type of mesh used in this experiment is the unstructured mesh to reduce the processing load on the systems. The number of elements generated in this type of mesh is 574870.

F. SET-UP OF THE ANALYSIS

The type of solver used in this experiment is pressure based as the velocity is less than Mach 1. Steady flow is considered as no shockwaves are involved. Spalart-Allmaras (vorticity-based) viscous model is chosen. The material is air and the density of 1.225 kg/ms.

TABLE 6: Boundary conditions.

x-inlet velocity	140 knots
z-inlet velocity	30 and 50 knots
Operating pressure	101325 Pascal
Temperature	300 k

Table 6. represents the boundary conditions before the analysis appropriate for this experiment.

The scheme for solving the equations is second-order for more accurate results. The fluent is the Finite Volume Model to convert the differential equations (non-linear) to algebraic forms. The flow was solved until it reached the desired criteria of convergence. The pressure and velocity values are obtained for each case.

VI. ANALYSIS RESULTS

Case 1- 0° crab angle- 0° control surfaces (Main-rudder and Winglet-rudder) deflection.

TABLE 7: Case1.

-	Direction	Vector	(0	0	1)
(n)	Coefficients				
Pressure	Viscous	Total	Pressure	Viscous	Total
0.094761	-0.00107	0.093695	2.98E-05	-3.36E-07	2.95E-05
0.001734	-0.00022	0.001513	5.46E-07	-6.97E-08	4.76E-07
-2.7404	0.001552	-2.73885	-0.00086	4.89E-07	-0.000862575
-1.79222	0.000448	-1.79177	-0.00056	1.41E-07	-0.000564303
2.736568	-0.00283	2.733733	0.000862	-8.93E-07	0.000860964
1.80815	-0.00062	1.807527	0.000569	-1.96E-07	0.000569264
0.056957	1.64E-05	0.056974	1.79E-05	5.17E-09	1.79E-05
---	---	---	---	---	---
0.165547	-0.00273	0.162819	5.21E-05	-8.59E-07	5.13E-05

The first case of the analysis is performed for a normal cruising speed of 140 knots. There is no involvement of any crosswind in this condition. The deflections of the main-rudder and winglet-rudder is 0. The values of the net force and the other parameters are mentioned in table 7.

Case 2- 0° crab angle- 0° control surface deflection- 30 knots crosswind velocity.

TABLE 8: Case 2.

-	Direction	Vector	(0	0	1)
(n)	Coefficients				
Pressure	Viscous	Total	Pressure	Viscous	Total
30.890393	0.93639918	31.82679	0.009729	0.000295	0.010024
-0.29111259	0.13540393	-0.15571	-9.17E-05	4.26E-05	-4.90E-05
-3.8274004	0.23171705	-3.59568	-0.00121	7.30E-05	-0.00113
4.3114336	0.01493172	4.326365	0.001358	4.70E-06	0.001363
6.0181968	0.30692838	6.325125	0.001895	9.67E-05	0.001992
12.781825	0.01244743	12.79427	0.004026	3.92E-06	0.004029
63.453288	0.0178064	63.47109	0.019984	5.61E-06	0.01999
---	---	---	---	---	---
113.33662	1.6556341	114.9923	0.035694	0.000521	0.036216

In the second case, the control surfaces' deflection remains 0° for 0° crab angle. The crosswind velocity of 30 knots is introduced in this condition. The net force value drastically increases compared to the first case. The first and second cases are done just to compare the net force values without the employment of control surfaces, with and without crosswind being introduced.

Case 3- 12° crab angle- 0° control surface deflection- 30 knots crosswind velocity.

International Journal of Engineering Research & Technology (IJERT)
ISSN: 2278-0181
Vol. 9 Issue 05, May-2020

TABLE 9: Case 3.

-	Direction	Vector	(0	0	1)
(n)	Coefficients				
Pressure	Viscous	Total	Pressure	Viscous	Total
11.44719	1.117859	12.56505	0.003605	0.000352	0.003957246
0.048648	0.204625	0.253273	1.53E-05	6.44E-05	7.98E-05
-4.26853	0.309156	-3.95937	-0.00134	9.74E-05	-0.001246967
-1.81515	0.037958	-1.77719	-0.00057	1.20E-05	-0.000559711
5.999249	0.389694	6.388943	0.001889	0.000123	0.002012139
6.863505	0.050497	6.914002	0.002162	1.59E-05	0.002177501
17.16744	0.162642	17.33008	0.005407	5.12E-05	0.005457949
---	---	---	---	---	---
35.44235	2.27243	37.71478	0.011162	0.000716	0.011877923

The case 3 represents the 12-degree crab angle given to the aircraft model. The control surface deflections remain zero with 30 knots crosswind velocity. The 12-degree crab angle is considered based on the table 9. When the aircraft was given a crab angle of 12-degrees, the force was reduced to a certain extent due to the crabbing technique.

Case 4- 12° crab angle- 24° main-rudder deflection- 30 knots crosswind velocity.

TABLE 10: Case 4.

-	Direction	Vector	(0	0	1)
(n)	Coefficients				
Pressure	Viscous	Total	Pressure	Viscous	Total
0.66968329	1.1145366	1.78422	0.000211	0.000351	0.000562
0.36948464	0.21917059	0.588655	0.000116	6.90E-05	0.000185
-4.2400678	0.30889945	-3.93117	-0.00134	9.73E-05	-0.00124
-2.1853638	0.0388662	-2.1465	-0.00069	1.22E-05	-0.00068
-12.44877	0.07638453	-12.3724	-0.00392	2.41E-05	-0.0039
6.0346621	0.3859939	6.420656	0.001901	0.000122	0.002022
6.4873002	0.05155357	6.538854	0.002043	1.62E-05	0.002059
-22.660698	0.1375392	-22.5232	-0.00714	4.33E-05	-0.00709
---	---	---	---	---	---
-27.973769	2.332944	-25.6408	-0.00881	0.000735	-0.00808

In the fourth case, with the given 12-degree crab angle, the main-rudder alone is deflected to 24-degrees along with 30 knots crosswind velocity. Only the main rudder is deflected, in this case, to prove the added advantages of the winglet-rudder. When the main-rudder is employed along with the crabbing angle of 12-degrees, the force is seen to have decreased compared to the case 3.

Case 5- 12° crab angle- 24° main rudder deflection- 50 knots crosswind velocity.

TABLE 11: Case 5

-	Direction	Vector	(0	0	1)
(n)	Coefficients				
Pressure	Viscous	Total	Pressure	Viscous	Total
16.80256	1.830385	18.63294	0.005292	0.000576	0.005868273
0.295292	0.332015	0.627307	9.30E-05	0.000105	0.000197565
-5.03417	0.47185	-4.56232	-0.00159	0.000149	-0.001436861
0.967797	0.051061	1.018858	0.000305	1.61E-05	0.00032088
-13.2999	0.086024	-13.2139	-0.00419	2.71E-05	-0.004161604
8.718207	0.637981	9.356188	0.002746	0.000201	0.002946645
15.23674	0.060219	15.29696	0.004799	1.90E-05	0.004817636
7.708056	0.1673	7.875356	0.002428	5.27E-05	0.002480271
---	---	---	---	---	---
31.39453	3.636834	35.03136	0.009887	0.001145	0.011032804

In the fifth case, the aircraft is given a crab angle of 12-degrees along with the main rudder deflection of 24-degrees. This condition unlike case-4 is for 50 knots. It is observed that the net force value after increasing the crosswind velocity to 50 knots also increases. The force has increased from negative value to positive value.

Case 6- 12° crab angle- 24° deflection of control surfaces- 50 knots crosswind velocity.

TABLE 12: Case 6

-	Direction	Vector	(0	0	1)
(n)	Coefficients				
Pressure	Viscous	Total	Pressure	Viscous	Total
16.455997	1.8445522	18.30055	0.005183	0.000581	0.005764
0.27977231	0.33688132	0.616654	8.81E-05	0.000106	0.000194
-0.51876122	0.0053355	-0.51343	-0.00016	1.68E-06	-0.00016
-5.0946611	0.47288859	-4.62177	-0.0016	0.000149	-0.00146
-0.37613777	0.04795744	-0.32818	-0.00012	1.51E-05	-0.0001
-13.218442	0.0843039	-13.1341	-0.00416	2.66E-05	-0.00414
-0.34633476	0.0055494	-0.34079	-0.00011	1.75E-06	-0.00011
8.4477136	0.64029917	9.088013	0.002661	0.000202	0.002862
12.78428	0.05890118	12.84318	0.004026	1.86E-05	0.004045
7.9841087	0.16679975	8.150909	0.002515	5.25E-05	0.002567
---	---	---	---	---	---
26.397535	3.6634685	30.061	0.008314	0.001154	0.009467

In the sixth case, the aircraft is given a crab angle of 12-degrees along with 24-degrees deflection from both the main-rudder and winglet-rudder. The crosswind velocity is 50 knots. After the employment of the winglet-rudder, it can be seen that the force has decreased from the fifth case. This case proves that the employment of the winglet-rudder adds helps in reducing the force which assists the aircraft to align itself nearer to the runway mid-line.

Case 7- 20° crab angle- 0° deflection of control surfaces- 50 knots crosswind velocity.

TABLE 13: Case 7

-	Direction	Vector	(0	0	1)
(n)	Coefficients				
Pressure	Viscous	Total	Pressure	Viscous	Total
12.6208	1.933783	14.55458	0.003975	0.000609	0.004583831
0.195294	0.356333	0.551627	6.15E-05	0.000112	0.00017373
-4.97397	0.514463	-4.45951	-0.00157	0.000162	-0.00140448
-3.67249	0.064422	-3.60807	-0.00116	2.03E-05	-0.001136327
8.040459	0.693469	8.733927	0.002532	0.000218	0.00275067
8.425606	0.106619	8.532225	0.002654	3.36E-05	0.002687146
12.64875	0.316405	12.96515	0.003984	9.96E-05	0.004083256
---	---	---	---	---	---
33.28445	3.985494	37.26994	0.010483	0.001255	0.011737825

In the above case, the crab angle is increased to 20-degrees for 50 knots of crosswind velocity. The control surfaces are not deflected and it remains zero. As the table represents, when the crab angle is increased to 50 knots, an increase in the force can be witnessed.

Case 8- 20° crab angle- 24° control surface deflections- 50 knots of crosswind velocity.

International Journal of Engineering Research & Technology (IJERT)
ISSN: 2278-0181
Vol. 9 Issue 05, May-2020

TABLE 14: Case 8

-	Direction	Vector	(0		0 1)
(n)	Coefficients				
Pressure	Viscous	Total	Pressure	Viscous	Total
-0.96205	1.989288	1.027241	-0.0003	0.000627	0.00032352
0.55658	0.384929	0.941509	0.000175	0.000121	0.00029652
-0.50193	0.006317	-0.49561	-0.00016	1.99E-06	-0.000156089
-5.051	0.524097	-4.52691	-0.00159	0.000165	-0.001425707
-5.45529	0.062571	-5.39272	-0.00172	1.97E-05	-0.001698386
-13.9188	0.109195	-13.8096	-0.00438	3.44E-05	-0.004349193
-0.78601	0.011069	-0.77494	-0.00025	3.49E-06	-0.00024406
8.134997	0.720578	8.855574	0.002562	0.000227	0.002788982
5.538956	0.107139	5.646095	0.001744	3.37E-05	0.001778186
-35.9555	0.264941	-35.6905	-0.01132	8.34E-05	-0.011240407
-48.4	4.180125	-44.2199	-0.01524	0.001316	-0.013926636

The eighth case is one of the most important condition that justifies the objective of this very paper. For a 20-degrees crab angle, and with 24-degrees of control surface deflections for a severe crosswind velocity of 50 knots; the force was decreased to a negative value. The crabbing angle along with the control surface deflections enables a safer landing for the amount of force obtained in this case.

Case 9- 20° crab angle- 30° control surface deflections- 50 knots of crosswind velocity.

TABLE 15: Case 9

-	Direction	Vector	(0	0	1)
(n)	Coefficients				
Pressure	Viscous	Total	Pressure	Viscous	Total
-0.65316555	1.961549	1.308383	-0.00021	0.000618	0.000412
0.62243276	0.38227911	1.004712	0.000196	0.00012	0.000316
-0.54780863	0.00561296	-0.5422	-0.00017	1.77E-06	-0.00017
-5.0371939	0.51464429	-4.52255	-0.00159	0.000162	-0.00142
-2.7637097	0.02005962	-2.74365	-0.00087	6.32E-06	-0.00086
-2.7353916	0.039539	-2.69585	-0.00086	1.25E-05	-0.00085
-14.054272	0.09719908	-13.9571	-0.00443	3.06E-05	-0.0044
-0.90909496	0.01053376	-0.89856	-0.00029	3.32E-06	-0.00028
8.2966824	0.70137038	8.998053	0.002613	0.000221	0.002834
0.6736989	0.0354818	0.709181	0.000212	1.12E-05	0.000223
4.4013046	0.06791141	4.469216	0.001386	2.14E-05	0.001408
-40.332606	0.25713024	-40.0755	-0.0127	8.10E-05	-0.01262
-53.039124	4.0933106	-48.9458	-0.0167	0.001289	-0.01542

The final case which suggests that on increasing the control surface deflections to 30-degrees which is the maximum deflection, the net force was further decreased from the previous case. The winglet-rudder configuration which is employed along with the main-rudder for crosswind landing conditions is thus proved to enable a safer landing.

VI. SUMMARY

Concerning to the analysis and the forces acting upon the aircraft, it can be concluded that-

1.0-degree deflection with 30 knots crosswind
a net positive pressure and viscous force is experienced on the aircraft and the value is quite higher than the sum of the forces experienced during the no deflection or 0-degree and 0 knots crosswind condition, without involving the mini rudder.

2. Further on involving a crab angle of 12 degrees with 24 degrees of 30 knots crosswind the positive forces seem to reduce than the previous case.

3. Analyzing the moments, sideways forces and the forces obtained in the x and z-direction it can be concluded that the involvement of the winglet rudder configuration along with the main rudder facing a 20-degree crab with 30-degree deflection in 50 knots fetches a favorable negative condition for a desirable landing or touchdown that is assisted by the mini rudder configuration using the crabbing technique.

4. The analysis proves that by adapting the crabbing technique during a severe crosswind condition along with the assistance of winglet-rudder configuration; enables a safer landing. The load on the rudder is reduced and assisted with helping overcome this critical landing condition.

VII. REFERENCES

[1] Al-shamma, O., Ali, R., & Hasan, H. S. (2018). "An Educational Rudder Sizing Algorithm for Utilization in Aircraft Design Software." International Journal of Applied Engineering Research, 13(10), 7889–7894.
[2] Bourdin, P., Gatto, A., & Friswell, M. I. (2008). "Aircraft control via variable cant-angle winglets." Journal of Aircraft, 45(2), 414–423. https://doi.org/10.2514/1.27720
[3] Fmky, P. (1977). /il (.. 40. "Stability and Control Characteristics of the Winglet Configures KC-135A."
[4] Hageman, R. (2016). "Rudder Incorporated Winglet Design for blended wing body aircraft." Delft University of Technology. http://repository.tudelft.nl/
[5] Theis, J., Ossmann, D., & Pfifer, H. (2017). "Robust Autopilot Design for Crosswind Landing." IFAC-PapersOnLine, 50(1), 3977–3982. https://doi.org/10.1016/j.ifacol.2017.08.770
[6] Zabihollah NAJAFIAN Ashrafi; Ahmad Sedghat. (2014). "Improving the Aerodynamic Performance of a Wing with Winglet." International Journal of Natural and Engineering Sciences, 8(6), 52–57.
[7] Soroush Akhgari, "Summary about crosswind in aviation and effect of crosswind on the airplane during landing" March 2016.